

1 **Semantic object-scene inconsistencies affect eye movements, but not in**
2 **the way predicted by contextualized meaning maps**

3

4 Marek A. Pedziwiatr^{1,2,*}, Matthias Kümmerer³, Thomas S.A. Wallis⁴, Matthias Bethge³, Christoph Teufel¹

5

6 ¹Cardiff University, Cardiff University Brain Research Imaging Centre (CUBRIC), School of Psychology, Cardiff, UK

7 ²Queen Mary University of London, Department of Biological and Experimental Psychology, London, UK

8 ³University of Tübingen, Tübingen, Germany

9 ⁴Technical University Darmstadt, Institute for Psychology and Centre for Cognitive Science, Darmstadt, Germany

10 * corresponding author: marek.pedziwi@gmail.com

11

12 **Abstract**

13 Semantic information is important in eye-movement control. An important semantic influence
14 on gaze guidance relates to object-scene relationships: objects that are semantically
15 inconsistent with the scene attract more fixations than consistent objects. One interpretation
16 of this effect is that fixations are driven towards inconsistent objects because they are
17 semantically more informative. We tested this explanation using contextualized meaning maps,
18 a method that is based on crowd-sourced ratings to quantify the spatial distribution of context-
19 sensitive ‘meaning’ in images. In Experiment 1, we compared gaze data and contextualized
20 meaning maps for images, in which objects-scene consistency was manipulated. Observers
21 fixated more on inconsistent vs. consistent objects. However, contextualized meaning maps
22 did not assigned higher meaning to image regions that contained semantic inconsistencies. In
23 Experiment 2, a large number of raters evaluated the meaningfulness of a set of carefully
24 selected image-regions. The results suggest that the same scene locations were experienced as
25 slightly less meaningful when they contained inconsistent compared to consistent objects. In
26 summary, we demonstrated that – in the context of our rating task – semantically inconsistent
27 objects are experienced as less meaningful than their consistent counterparts, and that
28 contextualized meaning maps do not capture prototypical influences of image meaning on
29 gaze guidance.

30

Introduction

31

32 Visual processing varies as a function of the retinal location at which a stimulus is presented:
33 with increasing eccentricity, processing is affected by crowding and a decrease in resolution
34 (see Rosenholtz, 2016 and Stewart et al., 2020 for reviews). Being able to rapidly move the
35 central parts of the eyes is therefore necessary to extract fine detail across large parts of the
36 visual field. Consequently, eye movements are critical for visual processing and it is important
37 to understand what processes underpin gaze guidance. Currently, the most popular framework
38 for answering this question assumes that the factors influencing human gaze allocation belong
39 to two broad categories: (i) image-computable features of the input processed in a bottom-up
40 fashion, and (ii) the internal states of the individual, such as knowledge or intentions, exerting
41 their influence in a top-down manner (Berga & Otazu, 2020; Henderson & Hayes, 2017;
42 Kollmorgen et al., 2010; Rothkopf et al., 2016).

43

44 Support for the notion that image-computable aspects of the input are important for the
45 guidance of eye movements comes from studies demonstrating that where humans look in
46 images can often be predicted by analyzing the visual features of these images (Borji et al.,
47 2013). Algorithms generating such predictions are called saliency models. Early saliency models,
48 such as GBVS (Harel et al., 2007), AWS (Garcia-Diaz, Fdez-Vidal, et al., 2012; Garcia-Diaz,
49 Leboran, et al., 2012) or the model by Itti and Koch (Itti & Koch, 2000; see also Krasovskaya &
50 MacInnes, 2019), attempted to maximize the accuracy of their predictions relying on simple
51 features such as intensity, color, and orientation contrasts. While the predictive power of these
52 models was moderate (Kümmerer et al., 2015), state-of-the-art saliency models, based on
53 powerful machine-learning algorithms called deep neural networks (see Storrs & Kriegeskorte,
54 2019 for review), can predict fixation locations much better than their predecessors while still
55 relying exclusively on image features (Kümmerer et al., 2017). One fundamental difference is
56 that while earlier models were based on parameter values determined by hand, current models
57 such as DeepGaze II (Kümmerer et al., 2016, 2017) or MSI-Net (Kroner et al., 2020) are based on
58 supervised learning, which does not require explicitly defined parameter values.

59

60 One limitation of all saliency-based approaches is their difficulty to account for factors in
61 oculomotor control that are not image-computable (Bayat et al., 2018; Bruce et al., 2015;

62 Henderson & Hayes, 2017; Pedziwiatr et al., 2021a; Tatler et al., 2011). For example, the fixation-
63 patterns of individuals viewing the same stimulus can vary as a function of their task and goals
64 (Hoppe & Rothkopf, 2019; Koehler et al., 2014; Rothkopf et al., 2016; Yarbus, 1967). Importantly,
65 however, oculomotor behavior is not constantly subjugated to a task; humans (and many other
66 animals) are intrinsically motivated to obtain information, and often move their eyes with no
67 purpose other than to explore the environment (Gottlieb & Oudeyer, 2018). Both early (Itti &
68 Koch, 2001) and more recent work (Adeli et al., 2017; Veale et al., 2017; Zelinsky & Bisley,
69 2015) argues that the oculomotor behavior exhibited in such ‘free-viewing’ conditions can be
70 largely explained by image-computable features.

71

72 This contention has not remained unchallenged. A number of studies demonstrated that even
73 when observers view images without a task, the spatial allocation of fixations can be guided by
74 factors which are not captured by current saliency models, namely, the semantic content of the
75 visual scene (Henderson et al., 2019; Peacock et al., 2019; Wu et al., 2014). One well-studied
76 semantic effect in eye movement research relates to object-scene consistency, where eye
77 movement behavior changes depending on the extent to which objects are semantically
78 consistent with the scene. In a seminal study (Loftus & Mackworth, 1978), one example
79 stimulus showed a farmyard scene either with a (semantically consistent) tractor, or a
80 (semantically inconsistent) octopus. Inconsistent objects such as the octopus were looked at
81 earlier, attracted more fixations, and were inspected for longer in comparison to consistent
82 objects. While some mixed results have since been found with respect to the timing of eye
83 movements (Wu et al., 2014), there is robust evidence demonstrating that object-scene
84 inconsistencies lead to more and longer fixations (Coco et al., 2020; Friedman, 1979; Henderson
85 et al., 1999; Öhlschläger & Võ, 2017; Pedziwiatr et al., 2021a).

86

87 Two primary mechanisms have been proposed to explain these effects. First, objects that are
88 viewed in inconsistent contexts are processed less effectively, as indicated by the drop in
89 recognition (Munneke et al., 2013) and detection (Biederman et al., 1982) performance (see
90 also Kaiser et al., 2019). Consequently, more fixations towards, and longer inspection times of
91 inconsistent objects are thought to reflect the increased resources needed to process these
92 stimuli (Bonitz & Gordon, 2008; Friedman, 1979). A second, and not mutually-exclusive,
93 explanation for the effects of object-scene inconsistencies on eye movements is based on the

94 notion that inconsistent objects are “more informative” (Loftus & Mackworth, 1978),
95 “semantically informative” (Henderson, 2011; Henderson et al., 1999), or “contain greater
96 meaning” (Peacock et al., 2019). According to this idea, people look at inconsistent objects in an
97 effort to maximize extraction of meaning from a scene.

98

99 This second interpretation has recently gained increased attention, in particular with the
100 development of meaning maps, a method to quantify the spatial distribution of ‘meaning’
101 across an image (Henderson & Hayes, 2017, 2018). Meaning maps are created by first
102 partitioning an image into many circular, partially-overlapping patches. These patches are
103 presented to individuals, who view them without knowing the scene from which they were
104 extracted (hence these maps are called context-free). Participants are asked to use a Likert
105 scale to “assess how “meaningful” an image is based on how informative or recognizable” they
106 think it is. Finally, these ratings are combined into a smooth distribution over the image to
107 create a map. Meaning indexed by this method has been demonstrated to be a better
108 predictor of fixations than a simple saliency model. This finding has been interpreted as
109 evidence that semantic information rather than image-computable features control eye
110 movements (Henderson & Hayes, 2017, 2018). The meaning map approach is rapidly gaining
111 popularity, and has been used to study eye movements in various contexts (listed in Henderson
112 et al., 2021).

113

114 A recent study evaluating the meaning map approach and comparing them to a wider range of
115 saliency models highlights some limitations of the method (Pedziwiatr et al., 2021a; see
116 Henderson et al., 2021 and Pedziwiatr et al., 2021b for ongoing debate). First, the findings
117 demonstrate that meaning maps are outperformed in predicting fixations by DeepGaze II
118 (Kümmerer et al., 2016, 2017), a saliency model based on a deep neural network, that indexes
119 high-level features rather than meaning. Second, it was found that meaning maps in their
120 original form do not ascribe more meaning to scene regions occupied by objects that are
121 semantically inconsistent with the global scene context compared to consistent objects
122 presented in the same region and matched in terms of low-level features. Together, the results
123 of this study led to the conclusion that there is so far no evidence that meaning maps measure
124 semantic information *per se* (for further discussion see Pedziwiatr et al., 2021b). Rather, they

125 might index visual features that can be correlated with semantics. In this respect, the original
126 form of meaning maps are similar to modern saliency models.

127

128 As detailed above, the original meaning maps ignore the global context of the scene – they are
129 created from ratings of isolated, ‘context-free’ image patches. To resolve this issue, Peacock et
130 al. (2019) recently proposed contextualized meaning maps to allow meaningfulness ratings to
131 capture global scene context effects, such as object-scene inconsistencies. Contextualized
132 meaning maps differ from the original meaning maps in one important detail: during rating,
133 each patch is presented alongside the full scene from which it originated. Therefore, raters
134 have access to the global scene context when assessing the meaningfulness of the patch.
135 Given the critical importance of context in scene semantics (Biederman et al., 1982; Võ et al.,
136 2019), contextualized meaning maps might be better suited to quantify semantic information
137 within visual scenes. Surprisingly, Peacock et al. (2019) found that contextualized meaning
138 maps predicted gaze density in a free-viewing task equally well as context-free meaning maps
139 (and both predicted gaze density better than the GBVS saliency model). They suggested,
140 however, that dissociations in prediction performance between context-free and
141 contextualized meaning maps might only occur for scenes containing object-scene
142 inconsistencies.

143

144 In the current study, we therefore assessed the extent to which contextualized meaning maps
145 are sensitive to semantic object-scene inconsistencies. Specifically, if inconsistent objects are
146 more meaningful (Henderson, 2011; Henderson et al., 1999; Loftus & Mackworth, 1978; Peacock
147 et al., 2019), then contextualized meaning maps should assign higher meaning to regions
148 occupied by them, and this should predict increased fixations on these objects (relative to
149 consistent objects). Using exactly the same procedure and instructions as Peacock and
150 colleagues (2019), we created contextualized meaning maps for two types of indoor scenes,
151 which were identical except for one object (Öhlschläger & Võ, 2017). This object was either
152 semantically consistent with the context, such as a hair brush on a bathroom sink, or the object
153 was replaced with an inconsistent object, such as a shoe on the sink. We conducted a detailed
154 analysis of these maps across scene types, and compared them to fixation patterns of human
155 observers.

156

157 To anticipate our findings, we demonstrate that contextualized meaning maps are not able to
158 predict the gaze changes elicited by the manipulation of semantic object-context consistency.
159 Moreover, our first experiment provided initial evidence that contextualized meaning maps
160 might attribute *less* meaning to scene regions that contain inconsistent compared to consistent
161 objects. Given this surprising result, in a second experiment, we asked a large number of raters
162 to provide meaningfulness ratings for a carefully controlled set of image patches. The results of
163 this second experiment replicated the surprising result from the first experiment, showing that
164 semantically inconsistent objects are judged as slightly less meaningful than consistent objects.
165 Overall, these results call for the assumptions of the meaning map approach to be
166 reconsidered.

167

168 **Methods and Results**

169

170 **Experiment 1**

171 The main goal of Experiment 1 was to assess the extent to which contextualized meaning maps
172 and human fixations are sensitive to local changes in semantic information within a scene,
173 resulting from the presence of objects that are semantically consistent vs. inconsistent with the
174 overall scene-context. This experiment compares contextualized meaning maps to the data
175 collected in (Pedziwiatr et al., 2021a); therefore, more methodological details on the stimuli and
176 eye movement data can be found in that report.

177

178 **Stimuli**

179 The stimulus set consisted of photographs of 36 indoor scenes, taken from the SCEGRAM
180 dataset (Öhlschläger & Võ, 2017). Each scene was photographed in two conditions: Consistent
181 and Inconsistent, resulting in two images per scene (72 images in total). Images from the
182 Consistent condition contained only objects that are typical for a given scene context. In the
183 Inconsistent condition, one of these objects was replaced with an object unusual in the context
184 provided by the whole scene, thus introducing a semantic inconsistency. For example, in one of
185 the scenes, a hair brush on a bathroom sink (Consistent condition) was replaced with a flip-flop
186 (Inconsistent condition) – see Fig. 1A. The SCEGRAM dataset is constructed in such a way that,
187 across scenes, consistent and inconsistent objects are matched for low-level properties
188 (Öhlschläger & Võ, 2017). In each scene, consistent and inconsistent objects occupy the same

189 image locations, and the superposition of the bounding boxes of both conditions constituted
190 what we call a Critical Region. These Critical Regions are important for the data analyses we
191 report further below because they contain the only image regions that differ between
192 conditions.

193

194 **Eye-movement data**

195 For all 72 images, we collected eye-tracking data from a group of 20 observers. Each observer
196 free-viewed the full set of images displayed in a random order while their eyes were tracked
197 with an EyeLink 1000+ eye-tracker. The images had a width of 688 pixels and a height of 524,
198 corresponding to, respectively, 19.7 and 15 degrees of a visual angle. Each image was presented
199 for 7 seconds, which is similar to the presentation duration of 8 s used in the original
200 contextualized meaning maps study (Peacock et al., 2019).

201

202 To analyze the eye-movement data, fixation locations were extracted from raw eye-tracker
203 recordings using a standard EyeLink algorithm. The discrete fixations on each image were
204 transformed into continuous distributions by means of Gaussian smoothing (filter cut-off
205 frequency: -6 dB; implemented in Matlab – see Kümmerer et al., 2020) followed by a
206 normalization to the [0-1] range.

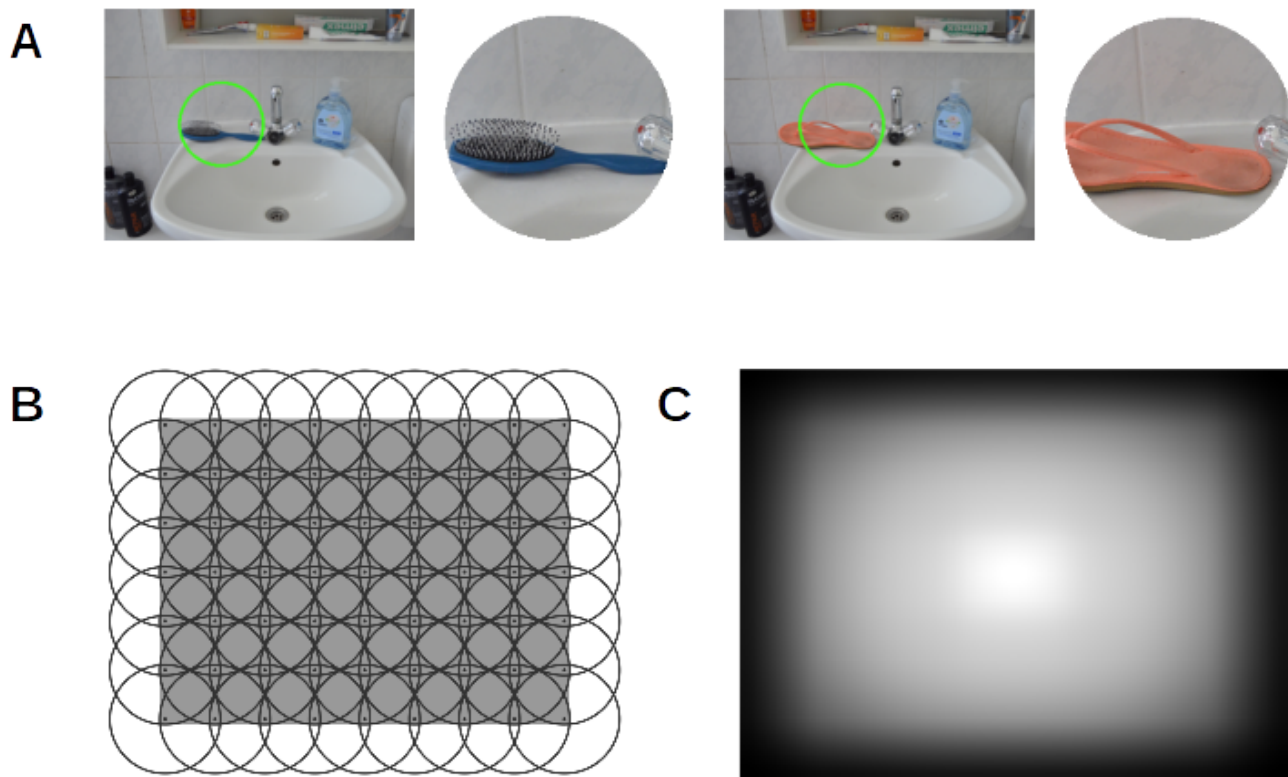
207

208 **Creating contextualized meaning maps – overview**

209 The procedure of creating contextualized meaning maps is identical to that used to generate
210 the original meaning maps except that raters see the entire original image alongside the patch
211 that they are asked to rate. We closely followed the procedure described in detail in previous
212 publications (Henderson & Hayes, 2017, 2018; Peacock et al., 2019; Pedziwiatr et al., 2021). In
213 summary, a pre-defined grid is used to segment the image into circular, partially overlapping
214 patches (Fig. 1B). Next, in a crowd-sourced online experiment, each patch is presented next to
215 the image from which it was derived, and human raters are asked to rate the meaningfulness
216 of the patch. Presenting the full image next to the patch ensures that the rater has access to
217 the scene context when providing their responses (Fig. 1A; see this figure for details of the
218 rating procedure itself). Each individual patch is rated by three individuals. In our study, we
219 used the same instructions for raters as the original contextualized meaning maps study
220 (retrieved from <https://osf.io/654uh>). Specifically, human raters were asked to rate how

221 ‘meaningful’ a patch is on a six-point Likert scale given how “informative or recognizable” they
222 find it (see caption for panel A on Fig. 1 for details). To provide raters with anchoring points for
223 their ratings, they viewed examples of patches during the instructions that should be rated as
224 low or high (again, the same as in the study by Peacock et al., 2019). After data collection, the
225 ratings from individual patches are combined into a smooth distribution over the image by
226 means of averaging and interpolation. For each image, these three steps are conducted twice:
227 once for bigger ‘coarse’ patches and once for smaller ‘fine’ patches. The maps resulting from
228 coarse and fine patches are averaged. Finally, the regions of the average map close to the
229 edges of the image are down-weighted (Fig. 1C). This manipulation accounts for the center-bias
230 of human eye-movements, i.e., the tendency to look more at the central region of an image
231 (Tatler, 2007).

232



233 Fig. 1. Generating contextualized meaning maps. A) Sample stimuli from the patch-rating task
234 used for creating contextualized meaning maps. The patch, which raters were asked to rate for its
235 meaningfulness, was always presented next to the image from which it originated to provide the
236 relevant context. A green circle on the context image indicated the location of the patch. Both
237 panels show the same scene, photographed in the Consistent (left part of the panel) and in the
238 Inconsistent (right part) condition. The images on both panels differ only with respect to the

239 object shown in the patch. The hair brush on the left part is a semantically consistent object for a
240 bathroom scene, the shoe on the right part is semantically inconsistent. In the task, raters were
241 asked to assess the meaningfulness of the patches based on their informativeness and
242 recognizability by means of selecting a value on a six-point rating scale. B) Grid used to segment
243 images into coarse patches. Grey rectangle represents image area. C) Center bias model used in
244 contextualized meaning maps. To account for the human tendency to allocate fixations
245 predominantly to central image-regions (a so-called center bias), contextualized meaning maps
246 assign different weights to different pixels of the maps depending on their location. This re-
247 weighting is done by computing a pixel-wise product between the maps and a model of center
248 bias shown on this panel, in which brighter pixels indicate higher pixel-weights. See Creating
249 contextualized meaning maps – modeling center-bias section for details.

250

251 **Creating contextualized meaning maps – parameter value selection**

252 When creating contextualized meaning maps for our stimuli, the aim was to match as closely as
253 possible the procedure used in the original study by Peacock and colleagues (2019). Our
254 images, however, differed in size from the stimuli used in that study and were viewed from a
255 different distance during the eye-movement data collection. In order to account for these
256 differences, we matched the two studies with respect to the size of coarse and fine patches in
257 degrees of visual angle (deg), and with respect to patch density of coarse and fine patches
258 expressed in the number of patches per square degree of visual angle (p/deg²). Under the
259 constraint that the centers of each two adjacent patches have to be equidistant horizontally
260 and vertically, these four values fully specify the grids necessary for creating contextualized
261 meaning maps. In terms of absolute values, matching the two studies with respect to these
262 parameters was perfect for patch diameter and resulted in 5.26 deg (coarse patches) and 2.26
263 deg (fine patches), which corresponded to 187 pixels and 79 pixels, respectively (205 and 87
264 pixels in the original study). The patch densities closest to the original we could possibly
265 achieve were 0.56 p/deg² and 0.21 p/deg² (compared to 0.57 p/deg² and 0.2 p/deg² in the original
266 study). Given the size of our stimuli, these values correspond to 63 coarse and 165 fine patches
267 per image. The resulting grid for creating coarse patches if shown on Fig. 1B.

268

269 **Creating contextualized meaning maps – data collection**

270 The procedure described in the previous sections resulted in a total of 16 416 patches (4 536
271 coarse and 11 880 fine patches). As described in more detail above and in the caption for Fig. 1,
272 each patch was rated for its meaningfulness by three human raters on a six-point Likert scale.
273 Patches were divided into 54 sets of 304 patches each, and each set was assigned to three
274 different raters (see details below).

275

276 Recall that each scene was photographed in a Consistent and an Inconsistent version, differing
277 only with respect to the identity of a single object. If the raters were to view the same scene in
278 both versions, there would be a high chance that they might guess the main focus of the study
279 and, in turn, adjust their rating strategy (by, for example, conditioning all rating values on the
280 presence – or absence – of the semantic inconsistency in the context image). To ensure that
281 meaning maps in scene pairs were independent, we assigned patches to sets in such a way that
282 each rater never saw the same scene in both the Consistent and Inconsistent conditions.
283 Specifically, we divided all the patches into two subsets. The first contained half of the patches
284 from the Consistent condition and half from the Inconsistent, with the patches in both these
285 halves derived from different scenes. The other subset contained the remaining patches.
286 Patches in each set presented for rating were always drawn only from one of these subsets.
287 Within each subset, patches were allocated to the Consistent and Inconsistent condition
288 randomly. Because of this division, raters were never exposed to the same scene in both
289 conditions but each rater was still exposed to scenes with and without semantic
290 inconsistencies.

291

292 Each set was rated by three unique raters, and 162 raters were recruited in total. The order of
293 patch presentation was randomized for each rater separately. Data collection was conducted
294 online. The raters were recruited using the crowdsourcing platform Prolific (www.prolific.co)
295 and the patch-rating task was implemented as a Qualtrics survey (Qualtrics, Provo, UT). All our
296 raters had to meet the following eligibility criteria: they had to be of U.S. nationality (as in the
297 original contextualized meaning maps study), they had to have submitted at least 100 tasks to
298 Prolific before, had to have an approval rate of 95% or more, and had to use a laptop or a
299 personal computer to complete the task. They were financially reimbursed for their time and
300 were allowed to participate in our study only once. Median completion time was 17.08 minutes
301 (interquartile range: 9.19).

302

303 **Creating contextualized meaning maps – modeling center-bias**

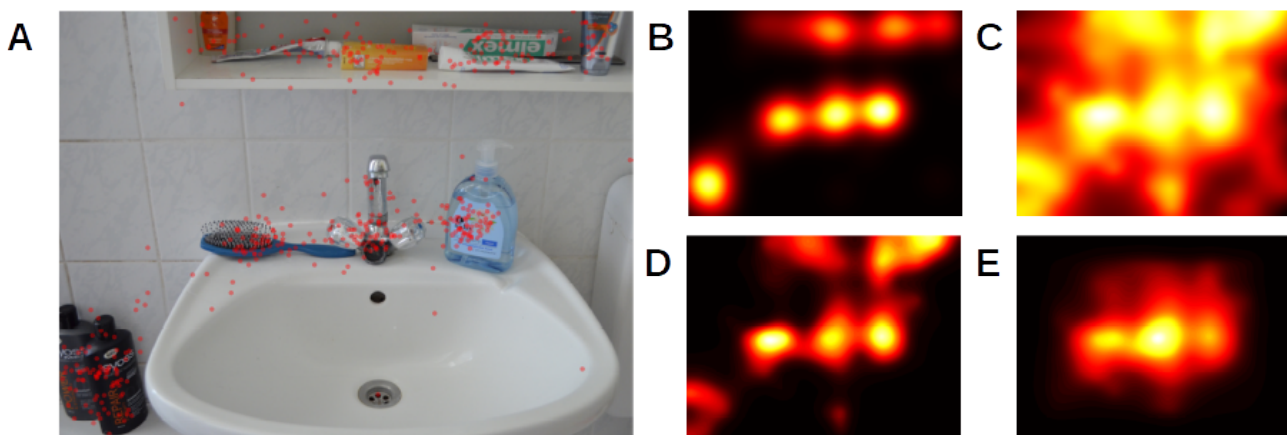
304 Recall that the final step of creating contextualized meaning maps involves reweighting the
305 map with a model of center bias. Such models have the form of smooths distributions over the
306 image, with higher values closer to the image center (Clarke & Tatler, 2014). When creating
307 contextualized meaning maps, we followed the original authors and relied on a model provided
308 with the saliency model GBVS (Harel et al., 2007; to be precise, we used the inverse of the
309 center-bias model included in the *invCenterBias.mat* file; inversion was achieved by subtracting
310 all values from one). This model is shown on Fig. 1C, its effects are illustrated on Fig. 2D and E.

311

312 **Creating contextualized meaning maps – histogram matching**

313 For each image, we matched the histogram of its contextualized meaning map to the
314 histogram of the distribution obtained by smoothing human fixations registered on this image.
315 This was done using the *imhistmatch* Matlab function. Histogram matching – also used in the
316 original meaning maps studies – ensures that values from both distributions are directly
317 comparable because they have been aligned to the same scale (see Fig. 2B, C, D). Similarly, as in
318 the original study by Peacock et al. (2019), this operation was conducted after including the
319 center-bias model in the maps.

320



321 *Fig. 2 Gaze data and outcomes of selected steps of creating a contextualized meaning map for an*
322 *example scene. A) Singles scene from the Consistent condition of our study, with fixations marked*
323 *with red dots. B) Smoothed fixations from panel A). The histogram of this distribution served as a*
324 *reference to which the histogram of the contextualized meaning map was matched. This*

325 procedure ensures the comparability of values from both distributions by aligning these values to
326 the same scale. C) ‘Raw’ contextualized meaning map for the scene from panel A). Since this map
327 has not been subjects to histogram matching, color values are not comparable to values on the
328 remaining panels. D) The map from panel C), after histogram matching but without including
329 center bias. Interestingly, contextualized meaning maps were better predictors of fixations when
330 they did not include the center bias (see Soundness check 1: general predictive power of
331 contextualized meaning maps section). E) The map from panel C), after application of the center-
332 bias model and subsequent subjection to histogram matching. Such maps were used in all our
333 analyses (unless otherwise stated) because we aimed to follow the original procedure.

334

335 **Data analysis software**

336 Data from this study was handled using Matlab R2020a (Mathworks Inc., Natick, MA) and R (R
337 Core Team, 2020). In particular, we relied on the R packages belonging to the tidyverse
338 collection (Wickham et al., 2019), as well as on packages jmv (The jamovi project, 2020; for
339 running ANOVAs) and ggExtra (Attali & Baker, 2019; for generating density plots presented on
340 Figures 5 and 6). Other R packages we used are cited in the relevant places in the text.

341

342 **Data and code availability**

343 The eye movement data used in this study are openly accessible via the following link:
344 <https://zenodo.org/record/3490434>). SCEGRAM stimuli are available under the following link:
345 <https://www.scenegrammarlab.com/research/scegram-database>. We also share all patch-rating
346 data and scripts for reproducing the results reported in this paper, as well as scripts and
347 instructions for creating contextualized meaning maps (links to be provided upon publication).

348

349 **Experiment 1 – Results**

350

351 **Soundness check 1: general predictive power of contextualized meaning maps**

352 As a soundness check, we tested how well contextualized meaning maps predicted human
353 fixations for our stimuli: we expected them to perform at least as well as in the original study
354 (Peacock et al., 2019). To quantify their predictive power, we applied a standard technique
355 (Bylinskii et al., 2019), used also by Peacock and colleagues (Peacock et al., 2019): for each
356 image, we calculated the correlation between its contextualized meaning map and smoothed

357 fixations registered on this image. For images from the Consistent condition, the average per-
358 image correlation was 0.60 (SD = 0.17). The average percent of the explained variance in the
359 eye-movement data amounted to 39%. In the Inconsistent condition, contextualized meaning
360 maps performed slightly worse ($M = 0.57$, $SD = 0.20$, 37% of the variance explained).
361 Additionally, we investigated the effects of removing center bias from contextualized meaning
362 maps and, interestingly, found that they performed better without it (Consistent: $M = 0.71$, $SD =$
363 0.13, 52% of the variance explained; Inconsistent: $M = 0.66$, $SD = 0.17$, 47% of the variance
364 explained).

365

366 Overall, these results are similar to what is reported in the original study (Peacock et al., 2019),
367 where the maps explained 40% of the variance in human data when center bias was included.
368 This finding thus provides an important soundness check for our study. A lower quality of
369 predictions in our study than in the original contextualized meaning maps study (Peacock et al.,
370 2019) could have indicated that either the procedure of creating contextualized meaning maps
371 is sensitive to aspects of the design which were different between our study and the original
372 study (such as absolute image size), or that there were some technical problems with our
373 implementation.

374

375 **Soundness check 2: comparing contextualized meaning maps to context-free meaning maps**

376 In our previous study (Pedziwiatr et al., 2021a), we generated original, context-free meaning
377 maps (Henderson & Hayes, 2017) for the scenes use in the Consistent condition in the current
378 study. As a second soundness check, we compared these original maps to the contextualized
379 meaning maps (note that this comparison was conducted on the maps without the center
380 bias). The average per-scene correlation between the two types of maps for the Consistent
381 condition was $M = 0.76$ ($SD = 0.12$). Regarding the ability to predict gaze patterns, the average
382 correlation with smoothed human-fixations was slightly higher for the context-free maps ($M =$
383 0.74, $SD = 0.14$ vs. $M = 0.71$, $SD = 0.13$; mean difference $M = 0.03$, $SD = 0.01$). The study that
384 introduced contextualized meaning maps (Peacock et al., 2019) also found that contextualized
385 and context-free meaning maps performed similarly in predicting fixations. Replicating this
386 finding provides another soundness check for our study.

387

388 Note that the exact parameter values determining the grids used to segment images into
389 patches differed slightly between the two types of meaning maps from our two studies. The
390 reason for this difference is that the reports introducing the original (Henderson & Hayes, 2017)
391 and contextualized (Peacock et al., 2019) meaning maps – on which we based our previous
392 (Pedziwiatr et al., 2021a) and present studies, respectively – differ with respect to the reported
393 sizes of images viewed by observers in the eye-tracking experiments (33×25 vs. 26.5×20
394 degrees of visual angle), yet use identical numbers of coarse and fine patches per image.

395

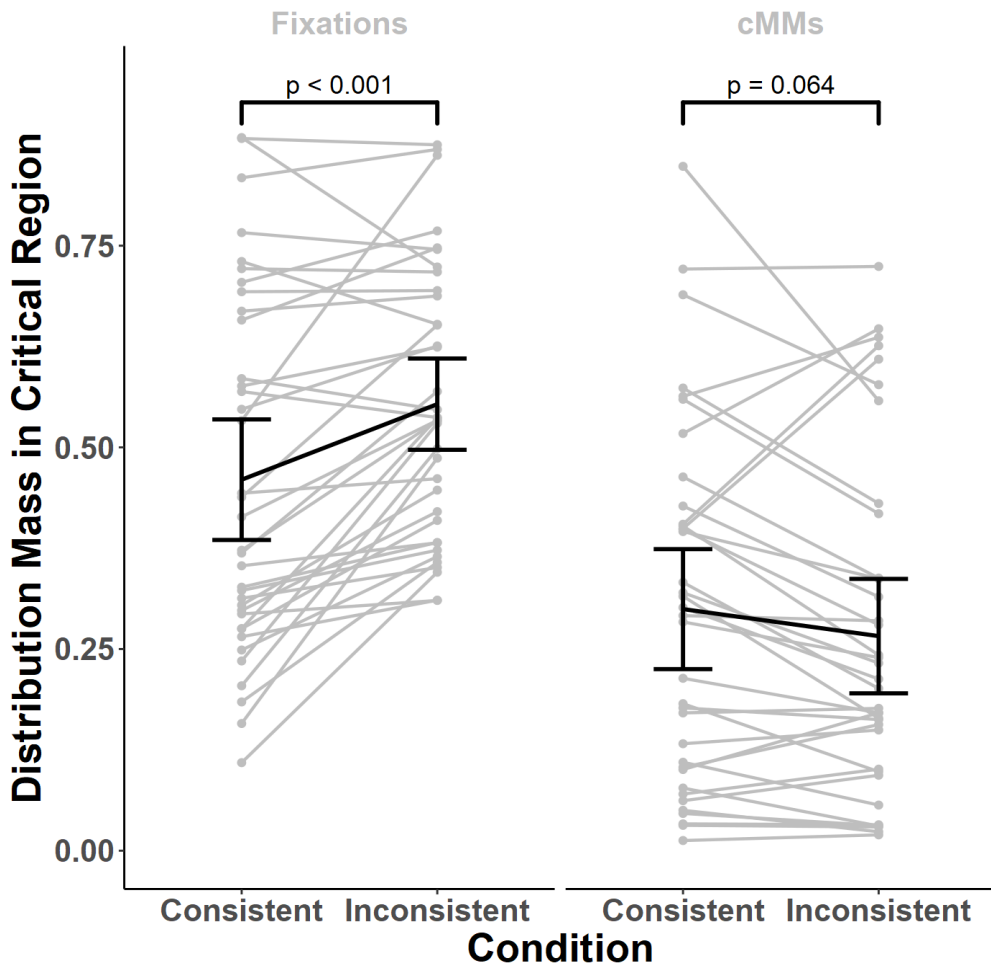
396 **Sensitivity of contextualized meaning maps and eye movements to semantic manipulations**

397 In our first main analysis, we compared contextualized meaning maps and smoothed human-
398 fixations with respect to their sensitivity to semantic manipulations. We focused on Critical
399 Regions – image regions which, depending on the condition, contained a semantically
400 consistent or inconsistent objects (see *Stimuli* section for details). For each scene, we first
401 performed histogram matching (see previous section) and then calculated the mass of each
402 distribution (contextualized meaning maps and smoothed fixations) falling within the Critical
403 Region and divided that value by the Region's area for normalization. These values were then
404 analyzed using a mixed 2×2 ANOVA with the condition (Consistent vs. Inconsistent) as a within-
405 subjects factor and the distribution source (contextualized meaning maps vs. smoothed
406 fixations) as a between-subjects factor (see Fig. 3). Please note that here a 'subject' indicates a
407 single scene. Such an approach is typical for studies comparing fixation-prediction methods and
408 is grounded in the observation that different observers agree to a large extent in their selection
409 of fixation targets in images (Kümmerer et al., 2015; Wilming et al., 2011).

410

411 This analysis revealed that both the distribution sources and conditions differed from each
412 other statistically (distribution source: $F(1, 70) = 23.05, p < 0.001, \omega^2 = 0.22$; condition: $F(1, 70) =$
413 $5.34, p = 0.024, \omega^2 = 0.003$). Importantly, however, these main effects were qualified by an
414 interaction ($F(1, 70) = 23.83, p < 0.001, \omega^2 = 0.02$). For post-hoc tests, we relied on non-
415 parametric paired Wilcoxon tests (as it is robust to the violations of the assumptions of
416 parametric tests we observed in the data), Bonferroni-corrected for two comparisons. These
417 tests showed that human eye-movements were sensitive to the change in semantic
418 relationship between object and scene, as indicated by the fact that more mass of the
419 smoothed-fixations distribution fell within the Critical regions in the Inconsistent condition

420 compared to the Consistent condition (Inconsistent - Consistent: $M = 0.09$, $SD = 0.12$, $p < 0.001$).
421 The same comparison, however, did not yield statistically significant differences for the
422 contextualized meaning maps ($M = -0.03$, $SD = 0.10$, $p = 0.064$). The hypothesis that
423 semantically-inconsistent regions carry more meaning was thus not supported by our data.
424 Indeed, the mean rating difference, though not significant due to the correction, was in the
425 opposite direction (consistent with the subsequent analyses and results we report below).
426



427 Fig. 3 Comparison of eye-movement data and contextualized meaning maps. In each condition and
428 for each scene, we calculated the amount of distribution-mass falling within the Critical Region
429 (the region, in which the manipulated objects were located) divided by the Region's area. This
430 calculation was performed separately for smoothed fixations and contextualized meaning maps.
431 Comparing these values between conditions revealed that observers tend to fixate the Critical
432 Regions more when they contained semantic inconsistencies (Inconsistent condition), as
433 compared to the situation when they did not (Consistent condition; left plot). Contextualized

434 meaning maps (right plot, labeled cMMs) did not show this effect, as they did not attribute more
435 meaning to semantic inconsistencies. In fact, they attributed numerically less meaning on average
436 but this effect was not significant in a statistical sense (but see Experiment 2). Each gray line
437 indicates a single scene, black oblique lines connect the means, black vertical lines indicate 95%
438 confidence intervals. *p*-values shown on the plot were obtained using paired Wilcoxon tests,
439 Bonferroni corrected for two comparisons.

440

441 Further analyses yielded unexpected findings. Recall that creating contextualized meaning
442 maps involved averaging the maps derived from coarse and fine patches. We repeated our
443 mixed ANOVA analysis separately for each of these maps. In both cases, the pattern of results
444 was similar to that reported in the previous section (fine maps: distribution source: $F(1, 70) =$
445 32.64 , $p < 0.001$, $\omega^2 = 0.26$, condition: $F(1, 70) = 0.08$, $p = 0.777$, interaction: $F(1, 70) = 31.56$, $p <$
446 0.001 , $\omega^2 = 0.04$; coarse maps: distribution source: $F(1, 70) = 41.85$, $p < 0.001$, $\omega^2 = 0.30$;
447 condition: $F(1, 70) = 3.71$, $p = 0.058$; interaction: $F(1, 70) = 5.87$, $p = 0.018$, $\omega^2 = 0.01$). In the post-
448 hoc tests, we did not find a difference between conditions for coarse maps (Inconsistent -
449 Consistent: $M = -0.01$, $SD = 0.23$, $p = 0.625$ uncorrected). Importantly, however, we obtained an
450 unexpected outcome in the post-hoc tests for the fine maps: these maps attributed less
451 meaning to Critical Regions in the Inconsistent condition than the Consistent condition
452 (Inconsistent - Consistent: $M = -0.08$, $SD = 0.15$, $p < 0.001$). Therefore, the numerical (but not
453 statistically significant) pattern observed at the level of full maps was most likely driven by the
454 fine maps component.

455

456 Note that these results were obtained using our custom-written, openly available
457 implementation of meaning maps (see *Data and code availability* section). To ensure that the
458 patterns we report above are not contingent on the specifics of our implementation, we
459 generated contextualized meaning maps using the code shared by the authors of the original
460 meaning maps and repeated our analyses with these maps. This code is available here:
461 <https://osf.io/654uh> (*build_meaning_map* function, version uploaded to the repository on
462 2020/01/18). The results showed a similar pattern: both the contextualized meaning maps and
463 their fine/coarse components attributed less meaning to the inconsistent objects (mean of the
464 differences for full maps: $M = -0.10$, $SD = 0.40$; coarse maps: $M = -0.07$, $SD = 0.56$; fine maps: $M =$
465 -0.14 , $SD = 0.46$; note that these values are not comparable to values reported in previous

466 analyses because here we used raw values from the *build_meaning_map* function). None of
467 these comparisons were statistically significant (full maps: $p = 0.304$; coarse maps: $p = 0.959$;
468 fine maps: $p = 0.082$), but for the fine maps this was because of Bonferroni correction for two
469 comparisons we applied (to remain consistent with the previous analyses). Together, this
470 analysis demonstrates that for both implementations, contextualized meaning maps do not
471 assign more meaning to semantically-inconsistent than consistent objects.

472

473 To summarize, human eye movements changed in response to local alterations in semantic
474 information: inconsistent objects attracted more fixations than consistent ones, and were
475 fixated earlier. Contextualized meaning maps and their coarse component did not show this
476 dependence on semantic information. Finally, fine maps ascribed *less* meaning to scene regions
477 when they contained inconsistent objects, which contradicts predictions from the meaning
478 map approach.

479

480 **Sensitivity of patch ratings to semantic manipulations**

481 Transforming patch ratings into contextualized meaning maps involves a number of steps,
482 including non-linear transformations. These steps could potentially mask real, or introduce
483 spurious between-condition differences, and for this reason, we conducted two analyses on
484 the raw rating data. In the first analysis, we selected all patches that had an overlap of at least
485 one pixel with the Critical Regions, and discarded the remaining patches. The ratings for
486 patches from each condition were averaged for each scene, separately for coarse and fine
487 patches. Averaging allowed us to account for between-scene differences in the number of
488 patches overlapping with Critical Regions and guaranteed that the data from each scene had
489 an equal contribution to the subsequent analyses. A comparison of these average ratings
490 between conditions provided no evidence to suggest that between-condition differences were
491 present in the raw data but were masked in the processes of assembling contextualized
492 meaning maps (see Table 1 rows 1 and 4).

493

494 Because the above analysis included patches with at least one pixel overlap with the bounding
495 boxes of objects, many of these patches showed only small parts of the manipulated objects,
496 or none at all. We therefore repeated this analysis with more stringent criteria for patch
497 inclusion. In order for a given patch to be included in this second analysis, the percentage of its

498 area overlapping with a Critical Region (dubbed Overlap Size henceforth) had to be above a
499 certain threshold (see Table 1). For patches of each size, we tested two threshold values. These
500 values were selected as 34th and 67th percentiles of all above-zero Overlap Size values. For the
501 first threshold, these values corresponded to 7% or more pixels of a patch overlapping with a
502 Critical Region for the coarse patches, and 18% for the fine patches. Similarly, the second
503 threshold corresponded to 21% and 56% or more overlapping pixels for coarse and fine patches,
504 respectively. The motivation for using percentiles to determine the thresholds was to make
505 sure that the consecutive analyses differ from each other by approximately the same
506 percentage of retained patches: while in the first analysis we included 100% of patches which
507 had above-zero Overlap Percentage, the thresholds resulted in including 66% (for 34th
508 percentile) and 33% (for 67th percentile) of them. For each threshold and each scene, we
509 averaged ratings of the retained patches, separately for each combination of experimental
510 condition and patch size, and compared these per-scene values between conditions (see Table
511 1 for full results). Only one of the resulting tests reached statistical significance: for the most
512 conservative threshold (i.e., with highest Overlap Size), fine patches from the Inconsistent
513 condition were rated as *less* meaningful than their equivalents from the Consistent one. The
514 magnitude of this difference was small: it amounted to 0.28 points on a scale from 1 to 6. The
515 remaining five comparisons exhibited the same directionality.

516

517 *Table 1: Comparison of patch ratings between conditions – statistical results*

Patch size	Percent of patches having above-zero Overlap Percentage included	Number of included scenes ¹	Mean difference in ratings (Inconsistent – Consistent) with 95% confidence intervals	Paired t-test results ²
Coarse	100%	36	-0.04 [-0.18; 0.09]	$t(35) = -0.63, p = 0.530$
	66%	35	-0.07 [-0.25; 0.11]	$t(34) = -0.78, p = 0.440$
	33%	27	-0.06 [-0.36; 0.25]	$t(26) = -0.38, p = 0.705$
Fine	100%	36	-0.02 [-0.13; 0.10]	$t(35) = -0.33, p = 0.747$
	66%	36	-0.05 [-0.21; 0.11]	$t(35) = -0.63, p = 0.533$
	33%	30	-0.28 [-0.54; -0.01]	$t(29) = -2.13, p = 0.042$

518

519 ¹Because some scenes had small Critical Regions, for more conservative thresholds none of the
520 patches derived from them had an Overlap Percentage high enough to be included in the
521 analysis.

522 ²We did not apply any correction for multiple comparisons here.
523

524 **Secondary analysis: prioritization of semantically inconsistent objects for fixation**

525 As a secondary point of interest, we examined the temporal evolution of the influences of
526 semantic inconsistencies on eye-movements. Other studies on the role of object-scene
527 consistency in eye movement control yielded conflicting findings regarding whether
528 inconsistent objects are fixated earlier or not (see Wu et al., 2014 for summary). In order to help
529 clarifying this issue, we compared, across experimental conditions, the number of fixations
530 required before the first fixations landed within the Critical Regions. On average, observers
531 took 5.03 fixations (SD = 4.7) to look at the inconsistent objects for the first time, and 5.97 (SD
532 = 5.55) for consistent (data pooled over scenes and observers). A paired Wilcoxon test
533 indicated that this difference was statistically significant ($p < 0.001$). The finding that the
534 inconsistent objects are not fixated immediately after image onset but still earlier than
535 consistent replicates the results of a recent study by Coco, Nuthmann and Dimigen (2020).
536 These authors supplemented gaze recordings with electroencephalography (EEG) and
537 concluded that object semantics can be at least partially accessed via peripheral vision.
538

539 **Summary of Experiment 1**

540 In our first experiment, we evaluated the extent to which contextualized meaning maps and
541 human eye-movements are sensitive to manipulations of the semantic relationship between
542 objects and scenes. Consistent with past literature, human observers looked more at objects
543 that are semantically inconsistent with the scene context compared to consistent objects.
544 Contrary to predictions of the meaning map approach, however, our results provided no
545 evidence that contextualized meaning maps assign more meaning to inconsistent than
546 consistent objects. This insensitivity to manipulations of semantic object-scene relationships
547 was already present at the level of the raw rating data, indicating it is not an artifact of the map
548 generation procedure.

549

550 When we analyzed only the contextualized meaning maps resulting from ratings on fine
551 patches, the maps assigned less ‘meaning’ to the Critical Region for inconsistent than
552 consistent objects; a similar effect was observed in the raw patch data. If robust, this result
553 would contrast with the explanation of the semantic inconsistency effect on eye movements
554 proposed by the meaning map approach. Given that the evidence from our first experiment
555 was based on a post-hoc subset analysis, we conducted a second experiment.

556

557 We considered two hypotheses for why we found statistically lower meaningfulness ratings for
558 inconsistent regions in only a subset of fine patches. Firstly, it could simply be a false positive.
559 Secondly, there might be a general but subtle tendency to rate semantic inconsistencies as less
560 meaningful, but the subtlety of this effect might have meant that it could not be detected in
561 ratings of coarse patches because of their low number (there were approximately 2.5 times
562 more fine as coarse patches). The goal of Experiment 2 was to adjudicate between these two
563 hypotheses. We created a single, well-controlled set of coarse patches derived from scenes
564 with consistent and inconsistent objects, and collected ratings from a substantially larger
565 sample of raters. If the reason we were unable to uncover the tendency to rate semantic
566 inconsistencies as less meaningful in the coarse patches was due to the low number of ratings
567 for these patches in Experiment 1, increasing the number of ratings in Experiment 2 should
568 allow us to find this effect even in coarse patches.

569

570 Experiment 2

571 Stimuli and design

572 In this experiment, we used the same 72 photographs (of 36 scenes) as in Experiment 1. For
573 each scene, we manually selected two coarse patches that fully contained the consistent and
574 inconsistent objects (see Fig. 4). The locations of these patches were the same in both
575 conditions but their content changed. These patches were dubbed Con and Incon. Con-patches
576 were derived from scenes in the Consistent condition, Incon in the Inconsistent condition. We
577 were primarily interested in the ratings associated with these two types of patches.

578

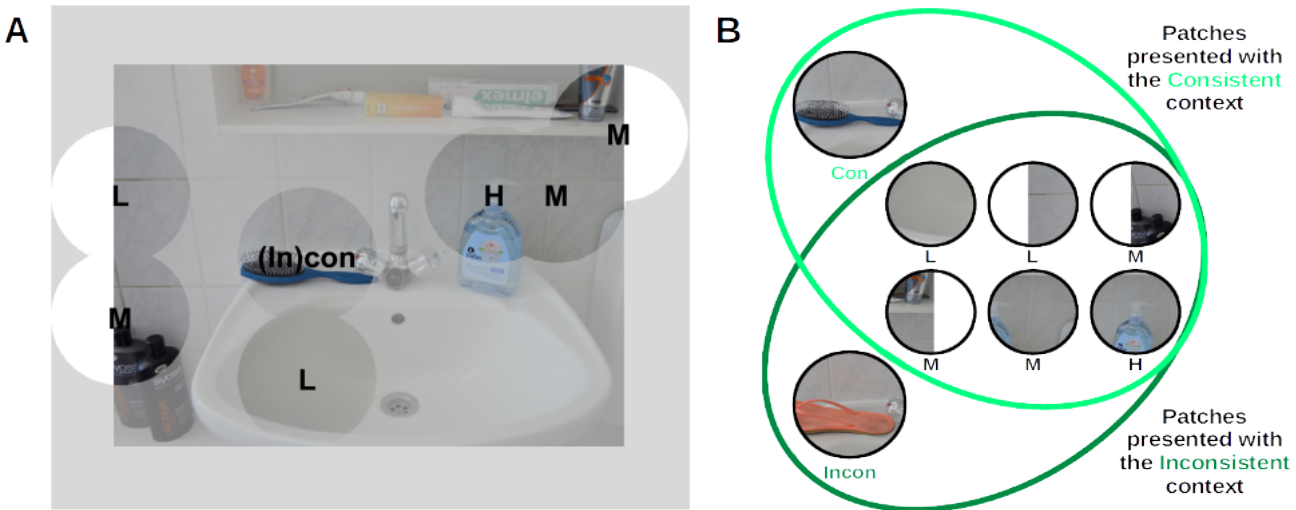
579 To mimic the variety of patches in the rating task used for creating contextualized meaning
580 maps and ensure that raters could use all values from the meaningfulness scale, we used the
581 ratings from Experiment 1 to select six additional patches from each scene (see Fig. 4): two

582 patches, which on average received the lowest meaningfulness ratings (dubbed L), one which
583 received the highest (dubbed H), and three patches for which the ratings were midway
584 between these extremes (dubbed M). This selection was carried out as follows. For each scene,
585 we considered all the coarse patches that had no overlap with the Critical Region. For each
586 location occupied by these patches, we averaged ratings across the Consistent and
587 Inconsistent conditions. We sorted the patches according to these average ratings in an
588 increasing order and selected two from the bottom (L), one from the top (H), and the three
589 closest to the median (M). Therefore, we selected eight patches for each scene in total: six
590 patches which were identical between conditions with respect to content (L, M, and H), and
591 two patches which differed (Con and Incon). Since we expected Con- and Incon-patches to be
592 rated as highly meaningful because they contain objects, we included only one H-patch but two
593 L-patches in order to encourage raters to use the different scale levels with approximately
594 equal frequency.

595

596 For stimulus presentation, each L-, M-, and H-patch was paired with the full images from both
597 conditions. In contrast, Con- and Incon-patches were paired only with either the consistent or
598 the inconsistent scenes, respectively. This resulted in a set of 504 patch-contexts pairs (36
599 scenes \times 2 conditions \times 6 L/M/H-patches + 36 Con-patches + 36 Incon-patches). We split this set
600 into two equally large subsets, each containing half of the patch-context pairs from one
601 condition and half from the other in order to avoid the situation that raters would be exposed
602 to the same scene in both conditions. Each rater would see one of the two subsets, and thus
603 provide ratings for 252 patches.

604



605 Fig. 4. Stimulus generation for Experiment 2. A, B) In the second experiment, we tested whether
606 patches depicting semantically inconsistent objects tend to be rated as less meaningful than their
607 counterparts depicting consistent objects. For each scene, we selected two patches containing the
608 consistent (Con) or the inconsistent (Incon) object. To mimic the context of the task used to
609 generate contextualized meaning maps, we additionally included six patches that did not differ
610 between photographs with consistent and inconsistent objects. These patches were chosen based
611 on ratings they received in Experiment 1: on average, they had been rated as either low in meaning
612 (labeled L on the figure, two patches), high (H, one patch) or midway between these extremes (M,
613 three patches). Some of the patches that were selected were close to image edges and were
614 therefore clipped. Similar to Experiment 1, each patch was presented next to either a consistent or
615 inconsistent context scene (see panel B).

616

617 **Sample-size justification**

618 For Experiment 2, we recruited 140 raters. This sample size was largely based on the amount of
619 resources we deemed reasonable for running this experiment. We planned to compare ratings
620 for Con- and Incon-patches for each rater as a paired comparison (after averaging over patches;
621 see below). After excluding 18 raters (see the *Rater inclusion criteria and inter-rater agreement*
622 section), the resulting sample-size of 122 raters allowed detecting effects having the magnitude
623 of Cohen's $D_z = 0.33$ with 95% power, when using paired, two-tailed t-test and when adopting a
624 significance level of 0.05 (as indicated by the G-Power 3.1 software; Erdfelder et al., 2009).

625

626 **Collecting meaningfulness ratings**

627 Data collection was conducted identically to Experiment 1. We used the same patch-rating task
628 (with the order of stimulus presentation randomized individually for each rater) and the same
629 method of recruiting raters (Prolific platform). The task completion times had a median of 16.12
630 minutes (interquartile range: 9.6).

631

632 **Rater inclusion criteria and inter-rater agreement**

633 We assumed that raters who followed the task instructions would agree in their ratings to a
634 large degree. For example, we assumed that they would consistently rate M-patches higher
635 than L-patches. Following that logic, we excluded raters whose ratings vastly disagreed with
636 the ratings provided by the majority of participants. We operationalized this idea by first
637 measuring the agreement of ratings within each possible pair of raters who had viewed the
638 same subset of patches using Krippendorff's α (A. F. Hayes & Krippendorff, 2007; Krippendorff,
639 1970). Values of α span from negative values to 1, where 1 indicates perfect agreement, 0
640 indicates the degree of agreement achievable by chance, and negative values indicate
641 systematic disagreement. We calculated pairwise α for our raters using the function `kripp.alpha`
642 from the R package `irr` (Gamer et al., 2019), with the option `scaleType` set to 'interval' (setting it
643 to 'ordinal' did not influence the pattern of results). Next, for each rater, we averaged the α
644 values from all pairs to which this rater belonged. These per-rater average α values (dubbed R_α
645 henceforth) indicated the degree to which a given rater agreed with other raters who rated the
646 same subset of patches. We visually inspected the histogram of R_α values calculated for all
647 raters and decided that in our final sample, we would include only raters having R_α larger than
648 0.40. This resulted in excluding 18 raters and retaining 122 (importantly, our main results do not
649 depend on this step – see *Influence of data exclusions* section). The average R_α for the retained
650 raters was 0.70 ($SD = 0.06$). Additionally, we calculated R_α values for the excluded raters only.
651 These values indicated the agreement being close to the chance level (mean = -0.06, $SD = 0.20$)
652 which means that these raters were most likely responding at random, rather than using a
653 common rating strategy, consistently differentiating them from the majority of our sample.

654

655 **Experiment 2 – Results**

656

657 **Patches that were manipulated between conditions (Con and Incon)**

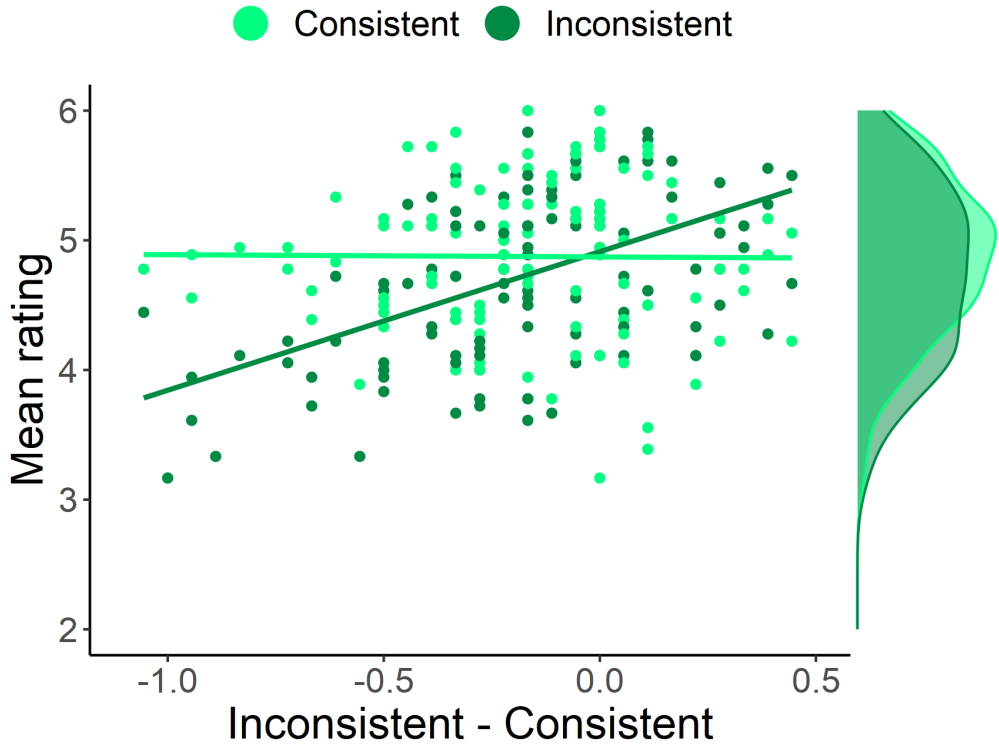
658 The main focus of Experiment 2 was to assess whether objects that are semantically
659 inconsistent with the scene context are rated differently with respect to the amount of
660 meaning they convey compared to consistent objects. Recall that each rater saw both Con- and
661 Incon-patches, but not the same scene in both conditions. We averaged ratings over patches in
662 each condition to yield a Con- and Incon-average rating for each rater, then compared them
663 with a paired-samples t-test. In line with the preliminary findings of Experiment 1, the results
664 demonstrate that semantically inconsistent objects were rated as less meaningful compared to
665 consistent objects. The absolute magnitude of this effect was small (mean of the differences: M
666 = -0.21, 95% CI [-0.14, -0.28]; median: -0.17) but statistically significant ($t(121) = 5.80$, $p < 0.001$).
667

668 To assess the contribution of the consistent vs. the inconsistent condition to this effect in a
669 subject-by-subject approach, we ordered the raters by the difference between their average
670 rating for Con- and Incon-patches. As shown in Fig. 5, this difference seems to be largely due to
671 changes in ratings of inconsistent patches: while there was no clear subject-by-subject
672 difference in the ratings for Con-patches, raters who contributed to the group-level effect
673 showed decreased ratings for D-Incon patches. This impression was corroborated by a
674 statistical analyses that showed a significant correlation between Con/Incon differences and
675 the Incon ratings ($r(111) = 0.52$, 95% CI [0.37; 0.64], $p < 0.001$), but no such relationship for Con
676 ratings ($r(111) = -0.01$, 95% CI [-0.19; 0.18], $p = 0.928$). Note that – for each analysis separately –
677 we excluded points which had a Cook's distance higher than 3 times the mean Cook distance
678 for all points. For Con ratings, this exclusion threshold amounted to 0.02 (0.03 for Incon) and
679 resulted in 9 exclusions (also 9 for Incon). We applied these exclusion criteria because the
680 initial inspection of the data suggested that, in each case, the effects might be driven by a small
681 number of points, which would have a disproportionately large influence on regression.
682 However, repeating the analyses with all the data included resulted in the same pattern of
683 outcomes (Incon: $r(120) = 0.50$, 95% CI [0.36; 0.62], $p < .001$; Con: $r(120) = -0.08$, 95% CI [-0.25;
684 0.10], $p = 0.398$).
685

686 These findings suggest that there is high consistency across raters regarding their evaluation of
687 the meaningfulness of objects that are semantically consistent with their scene context.
688 Ratings for inconsistent objects, in contrast, revealed considerable variability in rater behavior.
689 Different individuals tended to rate these objects as either lower, similar, or higher in meaning

690 than the consistent objects. Ultimately, this difference not only offers interesting insights into
691 individual differences but also suggests that the group-level effect is mainly driven by changes
692 in the ratings of inconsistent objects.

693



694 Fig. 5 *Meaningfulness ratings obtained for Con- and Incon-patches. For each rater, we averaged*
695 *ratings provided for Con-patches (light-green points) and for Incon-patches (dark-green points).*
696 *Next, we subtracted the average ratings for Incon-patches from Con-patches and ordered the*
697 *raters according to these difference scores. The ratings for Incon-patches, but not for Con-patches,*
698 *increase along this axis. Correlation analyses conducted for both types patches separately*
699 *confirmed this impression: the relationship between Con/Incon differences and ratings was*
700 *significant for the Incon-patches, but not for Con. Please note that this figure was generated using*
701 *data not containing points identified as outliers based on their Cook's distance (for details see*
702 *main text).*

703

704 Our final analysis focused on individual scenes, rather than individual raters, comparing ratings
705 for Con- and Incon-patches derived from the same scenes. For each scene, we conducted a
706 separate between-subjects Welch test comparing ratings received by Con- and Incon- patches,
707 similar to the analysis conducted for L/M/H-patches. Without correction for multiple

708 comparisons, 13 out of 36 of these tests yielded statistically significant results (this number was
709 reduced to 3 after applying the correction). Out of these 13 cases, in 12 (33% of all scenes) the
710 Incon-patch was rated as less meaningful than the Con-patch. These findings suggest that the
711 tendency of Incon-patches to be rated as less meaningful than Con-patches was observable at
712 the level of scenes too, which corroborates the finding from the rater-level analysis.

713

714 In summary, our main analyses demonstrate two key findings: first, we show that semantically
715 inconsistent objects are rated as less meaningful compared to consistent objects. Second, the
716 size of this effect shows marked individual differences between raters.

717

718 **Influence of data exclusions**

719 Recall that at the initial stage of our analyses we excluded 18 raters (see *Rater inclusion criteria*
720 and *inter-rater agreement* section). In order to make sure that our conclusions do not critically
721 depend on this step, we repeated all the analyses from the previous section with the data from
722 all raters recruited for Experiment 2. This operation did not change the pattern of our results
723 (comparison of ratings for Con- and Incon-patches: $t(139) = 5.99$, $p < 0.001$, mean of the
724 differences $M = -0.20$, 95% CI [-0.13; -0.27]; correlation for Con-patches: $r(138) = -0.10$, 95% CI [-
725 0.26; 0.07], $p = 0.242$; correlation for Incon-patches: $r(138) = 0.37$, 95% CI [0.21; 0.50], $p < 0.001$).

726

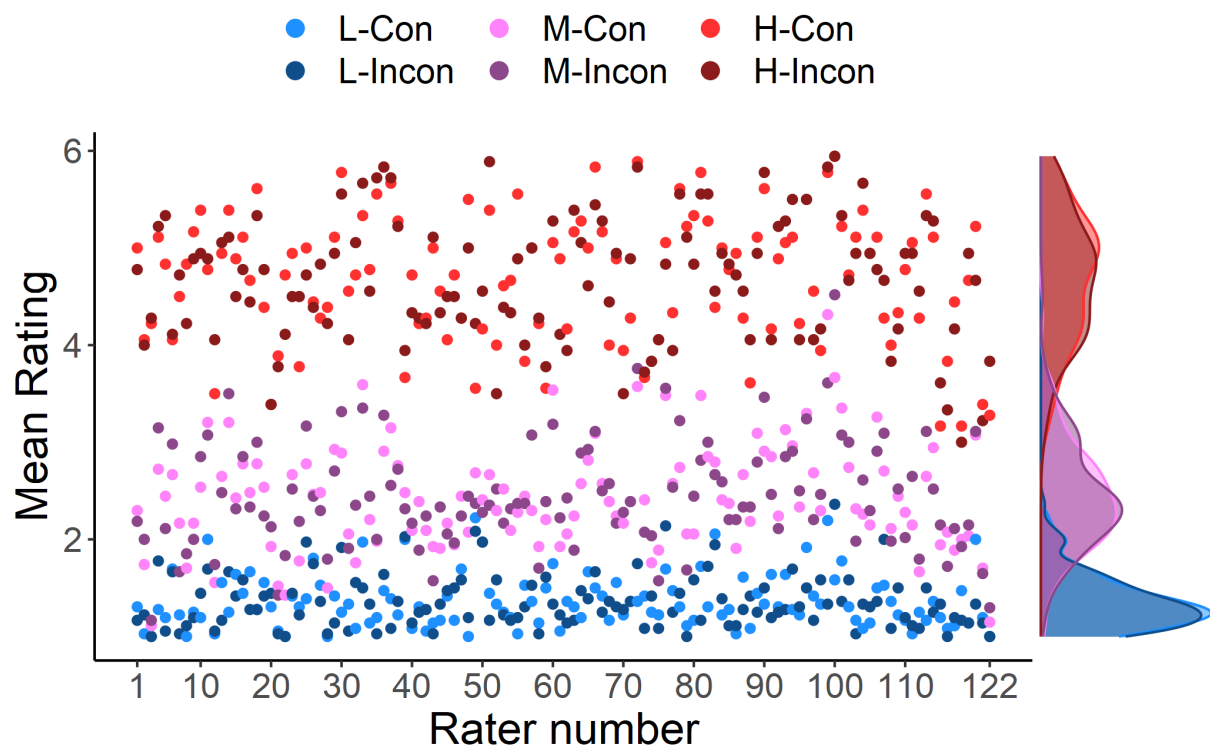
727 **Soundness check: patches that were identical between condition (L, M, and H)**

728 As a soundness check, we tested whether L, M, and H-patches were rated as low, medium and
729 high in meaning, respectively. We used Page's test, a non-parametric, rank-based statistical test
730 assessing the ordering of values obtained in repeated measurements (Page, 1963), and
731 compared the null hypothesis that there were no differences between ratings for all three
732 types of patches against the alternative stating that L-patches (mean rating $M = 1.36$, $SD =$
733 0.28) were rated lower than M-patches ($M = 2.44$, $SD = 0.55$) which, in turn, were rated lower
734 than H-patches ($M = 4.69$, $SD = 0.65$). We implemented the test with the R package crank
735 (Lemon, 2019) and conducted it separately for patches from the Consistent and the
736 Inconsistent conditions. In both cases the results were statistically significant (and identical
737 numerically: $L = 1708$, $p < 0.001$) which indicated that the pattern of obtained results matched
738 our expectations.

739

740 To evaluate whether the presence of consistent or inconsistent objects in a scene affect the
741 ratings for all patches in that scene, we analyzed whether ratings for L-, M-, and H-patches
742 differed between consistent and inconsistent conditions. For each rater, we averaged ratings
743 provided for each of these patch types per condition (see Fig. 6), and analyzed the averages
744 with a 2×3 repeated-measures ANOVA (with a Greenhouse-Geisser correction) with the two
745 within-subjects factors Condition (Consistent and Inconsistent) and Patch-Type (L-, M-, and H-
746 patches). As expected based on the preceding findings, this analysis also showed that ratings
747 differed according to patch type, as indicated by a main effect for this factor ($F(1.57, 190.25) =$
748 2530.65, $p < 0.001$). The other main effect and the interaction showed no significant differences
749 (Condition: $F(1, 121) = 0.02$, $p = 0.883$; interaction: $F(1.35, 163.16) = 0.77$, $p = 0.418$), showing that
750 average ratings for L-, M- and H- patches did not differ depending on whether the full scene
751 contained a consistent or inconsistent object.

752



753 Fig. 6. Meaningfulness ratings obtained for L-, M-, and H-patches, averaged per rater over scenes
754 and segregated by condition. Brighter colors indicate mean ratings from the Consistent condition,
755 darker from the Inconsistent. On the right-hand side, density plots are shown. Our analyses
756 revealed a statistically significant main effect of patch type (L, M, and H), but no effect of condition
757 or an interaction between condition and patch type.

758

759 In a final analysis of the L-, M-, and H-patches, we focused on potential differences between
760 individual scenes. The previous analyses reported in this section averaged patch ratings per
761 rater over scenes. In our final analysis, we took a different approach and compared ratings
762 provided for individual L-, M-, and H-patches across conditions. Individual patches were rated
763 by a separate set of raters in the Consistent and Inconsistent conditions (see section *Stimuli*
764 and *design* section). We therefore used a between-subjects Welch test to compare the ratings
765 for each patch individually across conditions and found statistically significant differences only
766 for 2 patches (out of 216), derived from 2 different scenes. Therefore, in the vast majority of
767 cases, the condition from which the context image was derived did not influence the ratings
768 for individual patches.

769

770 Overall, these control analyses have two implications. First, they indicate that the raters
771 adopted the expected rating strategy, as suggested by the expected ordering of values for L-,
772 M-, and H-patches. Second, exchanging a single object that is semantically consistent with the
773 scene for an inconsistent object did not have a general effect on the rating of patches that did
774 not contain the manipulated object, neither on average nor on a scene-by-scene level.

775

776 Discussion

777

778 Human fixations are attracted to objects that are semantically inconsistent with the scene
779 within which they appear. One possible explanation of these effects is that these objects carry
780 increased meaning, which causes people to look at them more. This hypothesis has gained
781 increasing attention with the development of meaning maps, a novel tool to index the
782 distribution of meaning across an image (Henderson & Hayes, 2017, 2018; Peacock et al., 2019).
783 In two experiments, we tested if semantically inconsistent objects indeed carry more meaning
784 as measured by contextualized meaning maps (Peacock et al., 2019), which have been designed
785 to capture such contextual effects. First, we created contextualized meaning maps for images
786 of scenes containing objects that were either semantically consistent or inconsistent, and
787 compared these maps to eye-movement data. While observers looked more at inconsistent
788 compared to consistent objects, contextualized meaning maps did not attribute higher
789 amounts of meaning to the former than to the latter. In fact, we found preliminary evidence to

790 suggest that the same scene location might be indexed as less rich in meaning when it contains
791 semantic inconsistency. In a second experiment, we therefore asked a substantially larger
792 number of raters to provide meaningfulness ratings for a carefully controlled set of image
793 patches, including patches that showed semantically consistent or inconsistent objects. The
794 results of this second experiment provide evidence suggesting that human observers have a
795 tendency to judge objects that are semantically inconsistent with the scene as slightly less
796 meaningful than their consistent counterparts.

797

798 The tendency of human observers to look more at semantically inconsistent objects is
799 considered to be a prototypical example of semantic influences on eye movements. Several
800 previous explanations of this effect implicitly or explicitly assume that semantic inconsistency
801 increases the amount of (semantic) information, or meaning that is conveyed (Henderson, 2011;
802 Henderson et al., 1999; Loftus & Mackworth, 1978). This interpretation has been strongly
803 expressed within the recently developed meaning map approach (Henderson & Hayes, 2017,
804 2018; Peacock et al., 2019 see also Henderson et al., 2019 for review). In contrast to this notion,
805 our direct evaluation of contextualized meaning maps suggests that, while they show a good
806 overall ability to predict human gaze patterns, they are unable to predict influences of semantic
807 inconsistencies, showing no difference between our Consistent and Inconsistent conditions.
808 Therefore, contextualized meaning maps fail to capture at least one context-based semantic
809 influence on eye-movement control.

810

811 It is important to highlight the fact that a conceptualization of meaning in terms of object-
812 context relationships is by no means exhaustive. Other conceptualizations have been proposed
813 (T. R. Hayes & Henderson, 2021; Hwang et al., 2011; Rose & Bex, 2020) and the idea that there
814 might be several subtypes of meaning that are important for eye movements has been
815 suggested by other authors (Henderson et al., 2018; Henderson & Hayes, 2018). Our findings
816 indicate that contextualized meaning maps and patch ratings do not capture the effect of
817 semantic object-scene relationships on eye movements, but they might measure other types of
818 meaning (see also Henderson et al., 2021). The critical question therefore is what type of gaze-
819 relevant meaning they might measure.

820

821 Answering this question is impeded by the fact that it is far from clear what raters are doing
822 when asked to provide meaningfulness judgments for image patches. In both experiments, we
823 used the instructions from the original contextualized meaning maps study by Peacock et. al
824 (2019). These instructions define meaningfulness in rather vague terms by linking it to
825 informativeness and recognizability. Raters are instructed as follows: “We want you to assess
826 how “meaningful” an image is based on how informative or recognizable you think it is”. Our
827 study shows that, at the group-level, such instructions lead to lower meaningfulness ratings for
828 objects that are semantically inconsistent with the scene context. One possible explanation for
829 this result is that raters find it more difficult to recognize inconsistent objects (“What is that on
830 the sink there? A shoe?”), and might therefore rate the meaningfulness of the patch lower
831 (emphasizing the “recognizable” component of the definition of meaningfulness used by the
832 meaning maps approach). Also note that the ambiguity of the instruction may cause higher
833 inter-subject variability in the inconsistent condition because raters might be unsure about how
834 to interpret the image manipulations in the context of the instructions.

835

836 Other instructions would likely lead to qualitatively different findings. For instance, imagine
837 observers were given identical instructions to those used in our study except that they were
838 also told that the images in the study show crime scenes. It seems plausible that raters would
839 pick out the semantically inconsistent objects as being particularly meaningful in this context
840 (emphasizing the “informative” aspect of the instruction). Adjusting task instructions (and,
841 potentially, the parameters of grids used for segmenting scenes into patches) systematically in
842 a wide range of cases in order to maximize the predictive power of the resulting maps might be
843 an interesting research direction. However, such an approach would entail treating meaning
844 maps not as a tool to measure the distribution of semantic information in scenes, but as
845 another method of predicting human fixations: a crowd-sourced saliency model. That is, a
846 method which prioritizes the quality of predictions over both the interpretability of
847 mechanisms generating these predictions (i.e. the ability to identify factors determining the
848 accuracy of predictions) and the explanatory power (i.e. the amount of gained insight into
849 human oculomotor control).

850

851 Alternatively, the variability in responses in the patch-ratings task in its current form makes this
852 task a potentially interesting tool for indexing individual differences (Hedge et al., 2018). While

853 we currently lack clarity regarding the processes underpinning the selection of rating values,
854 further research, combining the patch-rating task with other measures, might shed more light
855 on this issue, and thereby on individual differences in how the content of natural scenes is
856 processed. This topic is still understudied in the context of eye movements, despite the
857 evidence showing that such individual differences exist (De Haas et al., 2019; see also Kröger et
858 al., 2020).

859

860 Given the limitations of human rating data, current developments in computational approaches
861 might provide alternative methods that could contribute to a better understanding of the role
862 of high-level factors in eye-movement control, including semantic information and meaning. A
863 number of authors have attempted to develop indices of these high-level aspects of visual
864 input by applying techniques to images that have originally been developed in natural-language
865 processing (T. R. Hayes & Henderson, 2021; Hwang et al., 2011; Lüdecke et al., 2019; Rose &
866 Bex, 2020; Treder et al., 2020), in particular in the field of distributional semantics (Harris, 1954).

867 While these computational methods come with their own limitations, they have a number of
868 advantages over human rating data: they are comparably inexpensive, fast, and easy to use,
869 and can comfortably be applied to large image data sets due to their automation. Moreover,
870 computational tools have the potential to be less opaque compared to human rating data, and
871 might be more amenable to detailed analyses of which aspects of high-level scene content
872 contributes to eye-movement control. For instance, the finding that humans look more and
873 longer at semantically inconsistent objects might be based purely on a statistical analysis of
874 object co-occurrences in visual scenes (see Wang et al., 2010). Not surprisingly, recent analyses
875 of image datasets with more than 20 000 images indicate that different scene categories
876 indeed show a highly consistent clustering of object types (Treder et al., 2020), and the
877 oculomotor system might exploit these regularities for outlier detection. This interpretation of
878 the influence of object-scene inconsistencies on eye movements is similar in spirit to earlier
879 notions of saliency (Bruce & Tsotsos, 2009), but transfers this idea from a low-level (feature-
880 based) to a high-level (object- and scene-based) analysis of the visual input. While – most likely
881 – being an important contributor, co-occurrence *per se* does not necessarily amount to a
882 semantic relationship between objects, or meaning. And some computational approaches,
883 such as the one developed by Treder and colleagues (Treder et al., 2020), might have the
884 potential to determine whether oculomotor control relies purely on basic co-occurrence or

885 transforms these raw data further into a type of information that is closer to what we might
886 label ‘meaning’.

887

888 To summarize, introducing semantic inconsistencies to a scene region by replacing a
889 semantically consistent object with one that is semantically inconsistent did not increase the
890 amount of meaning attributed to this region by contextualized meaning maps, despite
891 increasing the number of human fixations landing on this region. Therefore, even though the
892 maps predicted human fixations well for scenes containing only consistent objects, they are
893 not able to account for semantic influences on human gaze-allocation linked to semantic
894 object-context inconsistencies. In fact, data from both of our experiments provide evidence
895 suggesting that human observers might have the tendency to rate semantically inconsistent
896 objects as slightly less meaningful than their consistent counterparts. Our results further
897 highlight the need for improved conceptualization and methods to investigate the role of
898 semantic information in human oculomotor control.

899

900

901 **CRediT author statement**

902 **M.P.:** Conceptualization, Methodology, Software, Investigation, Formal Analysis, Writing –
903 Original Draft, Writing – Review & Editing

904 **M.K., T.W., M.B.:** Conceptualization, Writing – Review & Editing

905 **C.T.:** Conceptualization, Formal Analysis, Resources, Writing – Original Draft, Writing – Review
906 & Editing, Supervision

907

908 **Acknowledgments**

909 We would like to thank Antje Nuthmann and Tom Freeman for their comments on an earlier
910 version of the manuscript. This work was supported by the German Federal Ministry of
911 Education and Research (BMBF): Tübingen AI Center, FKZ: 01IS18039A and the Deutsche
912 Forschungsgemeinschaft (DFG, German Research Foundation): Germany’s Excellence Strategy
913 – EXC 2064/1 – 390727645 and SFB 1233, RobustVision: Inference Principles and Neural
914 Mechanisms.

915

916

References

- 917
- 918 Adeli, H., Vitu, F., & Zelinsky, G. J. (2017). A Model of the Superior Colliculus Predicts Fixation
919 Locations during Scene Viewing and Visual Search. *The Journal of Neuroscience*, 37(6),
920 1453–1467. <https://doi.org/10.1523/JNEUROSCI.0825-16.2016>
- 921 Attali, D., & Baker, C. (2019). *ggExtra: Add Marginal Histograms to “ggplot2”, and More “ggplot2”*
922 *Enhancements* (version 0.9). <https://cran.r-project.org/package=ggExtra>
- 923 Bayat, A., Nand, A. K., Koh, D. H., Pereira, M., & Pomplun, M. (2018). Scene grammar in human
924 and machine recognition of objects and scenes. *IEEE Computer Society Conference on*
925 *Computer Vision and Pattern Recognition Workshops*, 2018-June(June), 2073–2080.
926 <https://doi.org/10.1109/CVPRW.2018.00268>
- 927 Berga, D., & Otazu, X. (2020). Modeling bottom-up and top-down attention with a
928 neurodynamic model of V1. *Neurocomputing*, 417, 270–289.
929 <https://doi.org/10.1016/j.neucom.2020.07.047>
- 930 Biederman, I., Mezzanotte, R. J., & Rabinowitz, J. C. (1982). Scene perception: Detecting and
931 judging objects undergoing relational violations. *Cognitive Psychology*, 14(2), 143–177.
932 [https://doi.org/10.1016/0010-0285\(82\)90007-X](https://doi.org/10.1016/0010-0285(82)90007-X)
- 933 Bonitz, V. S., & Gordon, R. D. (2008). Attention to smoking-related and incongruous objects
934 during scene viewing. *Acta Psychologica*, 129(2), 255–263.
935 <https://doi.org/10.1016/j.actpsy.2008.08.006>
- 936 Borji, A., Sihite, D. N., & Itti, L. (2013). Quantitative analysis of human-model agreement in visual
937 saliency modeling: A comparative study. *IEEE Transactions on Image Processing*, 22(1), 55–
938 69. <https://doi.org/10.1109/TIP.2012.2210727>
- 939 Bruce, N. D. B., & Tsotsos, J. K. (2009). Saliency, attention, and visual search: An information
940 theoretic approach. *Journal of Vision*, 9(3), 5–5. <https://doi.org/10.1167/9.3.5>
- 941 Bruce, N. D. B., Wloka, C., Frosst, N., Rahman, S., & Tsotsos, J. K. (2015). On computational
942 modeling of visual saliency: Examining what’s right, and what’s left. *Vision Research*, 116,
943 95–112. <https://doi.org/10.1016/j.visres.2015.01.010>
- 944 Bylinskii, Z., Judd, T., Oliva, A., Torralba, A., & Durand, F. (2019). What Do Different Evaluation
945 Metrics Tell Us About Saliency Models? *IEEE Transactions on Pattern Analysis and Machine*
946 *Intelligence*, 41(3), 740–757. <https://doi.org/10.1109/TPAMI.2018.2815601>
- 947 Clarke, A. D. F., & Tatler, B. W. (2014). Deriving an appropriate baseline for describing fixation
948 behaviour. *Vision Research*, 102, 41–51. <https://doi.org/10.1016/j.visres.2014.06.016>
- 949 Coco, M. I., Nuthmann, A., & Dimigen, O. (2020). Fixation-related Brain Potentials during
950 Semantic Integration of Object–Scene Information. *Journal of Cognitive Neuroscience*,
951 32(4), 571–589. https://doi.org/10.1162/jocn_a_01504

- 952 De Haas, B., Iakovidis, A. L., Schwarzkopf, D. S., & Gegenfurtner, K. R. (2019). Individual
953 differences in visual salience vary along semantic dimensions. *Proceedings of the National
954 Academy of Sciences of the United States of America*, 116(24), 11687–11692.
955 <https://doi.org/10.1073/pnas.1820553116>
- 956 Erdfelder, E., Faul, F., Buchner, A., & Lang, A. G. (2009). Statistical power analyses using
957 G*Power 3.1: Tests for correlation and regression analyses. *Behavior Research Methods*,
958 41(4), 1149–1160. <https://doi.org/10.3758/BRM.41.4.1149>
- 959 Friedman, A. (1979). Framing Pictures: The Role of Knowledge in Automatized Encoding and
960 Memory for Gist. *Journal of Experimental Psychology: General*, 108(3), 316–355.
961 <https://doi.org/10.1037/0096-3445.108.3.316>
- 962 Gamer, M., Lemon, J. and, Fellows, I., & Singh, P. (2019). *irr: Various Coefficients of Interrater
963 Reliability and Agreement* (version 0.84.1). <https://cran.r-project.org/package=irr>
- 964 Garcia-Diaz, A., Fdez-Vidal, X. R., Pardo, X. M., & Dosil, R. (2012). Saliency from hierarchical
965 adaptation through decorrelation and variance normalization. *Image and Vision Computing*,
966 30(1), 51–64. <https://doi.org/10.1016/j.imavis.2011.11.007>
- 967 Garcia-Diaz, A., Leboran, V., Fdez-Vidal, X. R., & Pardo, X. M. (2012). On the relationship between
968 optical variability, visual saliency, and eye fixations: A computational approach. *Journal of
969 Vision*, 12(6). <https://doi.org/10.1167/12.6.17>
- 970 Gottlieb, J., & Oudeyer, P.-Y. (2018). Towards a neuroscience of active sampling and curiosity.
971 *Nature Reviews Neuroscience*, 19(12), 758–770. <https://doi.org/10.1038/s41583-018-0078-0>
- 972 Harel, J., Koch, C., & Perona, P. (2007). Graph-Based Visual Saliency. In *Advances in Neural
973 Information Processing Systems* 19 (Vol. 19, pp. 545–552). The MIT Press.
974 <https://doi.org/10.7551/mitpress/7503.003.0073>
- 975 Harris, Z. S. (1954). Distributional Structure. *WORD*, 10(2–3), 146–162.
976 <https://doi.org/10.1080/00437956.1954.11659520>
- 977 Hayes, A. F., & Krippendorff, K. (2007). Answering the Call for a Standard Reliability Measure for
978 Coding Data. *Communication Methods and Measures*, 1(1), 77–89.
979 <https://doi.org/10.1080/19312450709336664>
- 980 Hayes, T. R., & Henderson, J. M. (2021). Looking for Semantic Similarity: What a Vector Space
981 Model of Semantics Can Tell Us About Attention in Real-world Scenes. *Psychological
982 Science*, In press. <https://doi.org/10.31219/osf.io/wsyz9>
- 983 Hedge, C., Powell, G., & Sumner, P. (2018). The reliability paradox: Why robust cognitive tasks
984 do not produce reliable individual differences. *Behavior Research Methods*, 50(3), 1166–
985 1186. <https://doi.org/10.3758/s13428-017-0935-1>

- 986 Henderson, J. M. (2011). Eye movements and scene perception. In S. P. Liversedge, I. D.
987 Gilchrist, & S. Everling (Eds.), *The Oxford Handbook of Eye Movements*. Oxford University
988 Press. <https://doi.org/10.1093/oxfordhb/9780199539789.013.0033>
- 989 Henderson, J. M., & Hayes, T. R. (2017). Meaning-based guidance of attention in scenes as
990 revealed by meaning maps. *Nature Human Behaviour*, 1(October).
991 <https://doi.org/10.1038/s41562-017-0208-0>
- 992 Henderson, J. M., & Hayes, T. R. (2018). Meaning guides attention in real-world scene images:
993 Evidence from eye movements and meaning maps. *Journal of Vision*, 18(6), 10.
994 <https://doi.org/10.1167/18.6.10>
- 995 Henderson, J. M., Hayes, T. R., Peacock, C. E., & Rehrig, G. (2019). Meaning and Attentional
996 Guidance in Scenes: A Review of the Meaning Map Approach. *Vision*, 3(2), 19.
997 <https://doi.org/10.3390/vision3020019>
- 998 Henderson, J. M., Hayes, T. R., Peacock, C. E., & Rehrig, G. (2021). Meaning maps capture the
999 density of local semantic features in scenes: A reply to Pedziwiatr, Kümmerer, Wallis,
1000 Bethge & Teufel (2021). *Cognition*, January, 104742.
1001 <https://doi.org/10.1016/j.cognition.2021.104742>
- 1002 Henderson, J. M., Hayes, T. R., Rehrig, G., & Ferreira, F. (2018). Meaning Guides Attention
1003 during Real-World Scene Description. *Scientific Reports*, 8(1), 13504. <https://doi.org/10.1038/s41598-018-31894-5>
- 1005 Henderson, J. M., Weeks, Phillip A., J., & Hollingworth, A. (1999). The Effects of Semantic
1006 Consistency on Eye Movements During Complex Scene Viewing. *Journal of Experimental
1007 Psychology: Human Perception and Performance*, 25(1), 210–228.
1008 <https://doi.org/10.1037/0096-1523.25.1.210>
- 1009 Hoppe, D., & Rothkopf, C. A. (2019). Multi-step planning of eye movements in visual search.
1010 *Scientific Reports*, 9(1), 144. <https://doi.org/10.1038/s41598-018-37536-0>
- 1011 Hwang, A. D., Wang, H.-C., & Pomplun, M. (2011). Semantic guidance of eye movements in real-
1012 world scenes. *Vision Research*, 51(10), 1192–1205. <https://doi.org/10.1016/j.visres.2011.03.010>
- 1013 Itti, L., & Koch, C. (2000). A saliency-based search mechanism for overt and covert shifts of
1014 visual attention. *Vision Research*, 40(10–12), 1489–1506. [https://doi.org/10.1016/S0042-6989\(99\)00163-7](https://doi.org/10.1016/S0042-
1015 6989(99)00163-7)
- 1016 Itti, L., & Koch, C. (2001). Computational modelling of visual attention. *Nature Reviews
1017 Neuroscience*, 2(3), 194–203. <https://doi.org/10.1038/35058500>
- 1018 Kaiser, D., Quek, G. L., Cichy, R. M., & Peelen, M. V. (2019). Object Vision in a Structured World.
1019 *Trends in Cognitive Sciences*, 23(8), 672–685. <https://doi.org/10.1016/j.tics.2019.04.013>

- 1020 Koehler, K., Guo, F., Zhang, S., & Eckstein, M. P. (2014). What do saliency models predict?
1021 *Journal of Vision*, 14(3). <https://doi.org/10.1167/14.3.14>
- 1022 Kollmorgen, S., Nortmann, N., Schröder, S., & König, P. (2010). Influence of low-level stimulus
1023 features, task dependent factors, and spatial biases on overt visual attention. *PLoS*
1024 *Computational Biology*, 6(5). <https://doi.org/10.1371/journal.pcbi.1000791>
- 1025 Krasovskaya, S., & MacInnes, W. J. (2019). Salience Models: A Computational Cognitive
1026 Neuroscience Review. *Vision*, 3(4), 56. <https://doi.org/10.3390/vision3040056>
- 1027 Krippendorff, K. (1970). Estimating the reliability, systematic error and random error of interval
1028 data. *Educational and Psychological Measurement*, 30, 61–70.
- 1029 Kröger, J. L., Lutz, O. H.-M., & Müller, F. (2020). What Does Your Gaze Reveal About You? On
1030 the Privacy Implications of Eye Tracking. In *IFIP Advances in Information and Communication*
1031 *Technology: Vol. 576 LNCS* (Issue March, pp. 226–241). Springer International Publishing.
1032 https://doi.org/10.1007/978-3-030-42504-3_15
- 1033 Kroner, A., Senden, M., Driessens, K., & Goebel, R. (2020). Contextual encoder–decoder
1034 network for visual saliency prediction. *Neural Networks*, 129, 261–270.
1035 <https://doi.org/10.1016/j.neunet.2020.05.004>
- 1036 Kümmerer, M., Bylinskii, Z., Judd, T., Borji, A., Itti, L., Durand, F., Oliva, A., & Torralba, A. (2020).
1037 *MIT/Tübingen Saliency Benchmark*. <https://saliency.tuebingen.ai/>
- 1038 Kümmerer, M., Wallis, T. S. A., & Bethge, M. (2015). Information-theoretic model comparison
1039 unifies saliency metrics. *Proceedings of the National Academy of Sciences*, 112(52), 16054–
1040 16059. <https://doi.org/10.1073/pnas.1510393112>
- 1041 Kümmerer, M., Wallis, T. S. A., & Bethge, M. (2016). *DeepGaze II: Reading fixations from deep*
1042 *features trained on object recognition*. <http://arxiv.org/abs/1610.01563>
- 1043 Kümmerer, M., Wallis, T. S. A., Gatys, L. A., & Bethge, M. (2017). Understanding Low- and High-
1044 Level Contributions to Fixation Prediction. *Proceedings of the IEEE International Conference*
1045 *on Computer Vision, 2017-Octob*, 4799–4808. <https://doi.org/10.1109/ICCV.2017.513>
- 1046 Lemon, J. (2019). *crank: Completing Ranks* (version 1.1-2).
1047 <https://cran.r-project.org/package=crank>
- 1048 Loftus, G. R., & Mackworth, N. H. (1978). Cognitive determinants of fixation location during
1049 picture viewing. *Journal of Experimental Psychology: Human Perception and Performance*,
1050 4(4), 565–572. <https://doi.org/10.1037/0096-1523.4.4.565>
- 1051 Lüddecke, T., Agostini, A., Fauth, M., Tamosiunaite, M., & Wörgötter, F. (2019). Distributional
1052 semantics of objects in visual scenes in comparison to text. *Artificial Intelligence*, 274, 44–
1053 65. <https://doi.org/10.1016/j.artint.2018.12.009>

- 1054 Munneke, J., Brentari, V., & Peelen, M. V. (2013). The influence of scene context on object
1055 recognition is independent of attentional focus. *Frontiers in Psychology*, 4(AUG).
1056 <https://doi.org/10.3389/fpsyg.2013.00552>
- 1057 Öhlschläger, S., & Võ, M. L.-H. (2017). SCEGRAM: An image database for semantic and syntactic
1058 inconsistencies in scenes. *Behavior Research Methods*, 49(5), 1780–1791.
1059 <https://doi.org/10.3758/s13428-016-0820-3>
- 1060 Page, E. B. (1963). Ordered Hypotheses for Multiple Treatments: A Significance Test for Linear
1061 Ranks. *Journal of the American Statistical Association*, 58(301), 216–230.
1062 <https://doi.org/10.1080/01621459.1963.10500843>
- 1063 Peacock, C. E., Hayes, T. R., & Henderson, J. M. (2019). The role of meaning in attentional
1064 guidance during free viewing of real-world scenes. *Acta Psychologica*, 198(December 2018),
1065 102889. <https://doi.org/10.1016/j.actpsy.2019.102889>
- 1066 Pedziwiatr, M. A., Kümmerer, M., Wallis, T. S. A., Bethge, M., & Teufel, C. (2021a). Meaning maps
1067 and saliency models based on deep convolutional neural networks are insensitive to image
1068 meaning when predicting human fixations. *Cognition*, 206(10), 104465.
1069 <https://doi.org/10.1016/j.cognition.2020.104465>
- 1070 Pedziwiatr, M. A., Kümmerer, M., Wallis, T. S. A., Bethge, M., & Teufel, C. (2021b). There is no
1071 evidence that meaning maps capture semantic information relevant to gaze guidance:
1072 Reply to Henderson, Hayes, Peacock, and Rehrig (2021). *Cognition, April*, 104741.
1073 <https://doi.org/10.1016/j.cognition.2021.104741>
- 1074 R Core Team. (2020). *R: A language and environment for statistical computing* (R-4.0.2). R
1075 Foundation for Statistical Computing. <https://www.r-project.org/>
- 1076 Rose, D., & Bex, P. (2020). The Linguistic Analysis of Scene Semantics: LASS. *Behavior Research
1077 Methods*, 52(6), 2349–2371. <https://doi.org/10.3758/s13428-020-01390-8>
- 1078 Rosenholtz, R. (2016). Capabilities and Limitations of Peripheral Vision. *Annual Review of Vision
1079 Science*, 2, 437–457. <https://doi.org/10.1146/annurev-vision-082114-035733>
- 1080 Rothkopf, C. A., Ballard, D. H., & Hayhoe, M. M. (2016). Task and context determine where you
1081 look. *Journal of Vision*, 7(14), 16. <https://doi.org/10.1167/7.14.16>
- 1082 Stewart, E. E. M., Valsecchi, M., & Schütz, A. C. (2020). A review of interactions between
1083 peripheral and foveal vision. *Journal of Vision*, 20(12), 2. <https://doi.org/10.1167/jov.20.12.2>
- 1084 Storrs, K. R., & Kriegeskorte, N. (2019). Deep Learning for Cognitive Neuroscience.
1085 <http://arxiv.org/abs/1903.01458>
- 1086 Tatler, B. W. (2007). The central fixation bias in scene viewing: Selecting an optimal viewing
1087 position independently of motor biases and image feature distributions. *Journal of Vision*,
1088 7(14). <https://doi.org/10.1167/7.14.4>

- 1089 Tatler, B. W., Hayhoe, M. M., Land, M. F., & Ballard, D. H. (2011). Eye guidance in natural vision:
1090 reinterpreting salience. *Journal of Vision*, 11(5), 5. <https://doi.org/10.1167/11.5.5>
- 1091 The jamovi project. (2020). *jamovi*. <https://www.jamovi.org>
- 1092 Treder, M. S., Mayor-Torres, J., & Teufel, C. (2020). *Deriving Visual Semantics from Spatial*
1093 *Context: An Adaptation of LSA and Word2Vec to generate Object and Scene Embeddings*
1094 *from Images*. <http://arxiv.org/abs/2009.09384>
- 1095 Veale, R., Hafed, Z. M., & Yoshida, M. (2017). How is visual salience computed in the brain?
1096 Insights from behaviour, neurobiology and modelling. *Philosophical Transactions of the*
1097 *Royal Society B: Biological Sciences*, 372(1714), 20160113.
1098 <https://doi.org/10.1098/rstb.2016.0113>
- 1099 Võ, M. L.-H., Boettcher, S. E., & Draschkow, D. (2019). Reading scenes: how scene grammar
1100 guides attention and aids perception in real-world environments. *Current Opinion in*
1101 *Psychology*, 29, 205–210. <https://doi.org/10.1016/j.copsyc.2019.03.009>
- 1102 Wang, H.-C., Hwang, A. D., & Pomplun, M. (2010). Object Frequency and Predictability Effects
1103 on Eye Fixation Durations in Real-World Scene Viewing. *Journal of Eye Movement Research*,
1104 3(3), 1–10. <https://doi.org/10.16910/jemr.3.3.3>

- 1105 Wickham, H., Averick, M., Bryan, J., Chang, W., McGowan, L., François, R., Grolemund, G.,
1106 Hayes, A., Henry, L., Hester, J., Kuhn, M., Pedersen, T., Miller, E., Bache, S., Müller, K.,
1107 Ooms, J., Robinson, D., Seidel, D., Spinu, V., ... Yutani, H. (2019). Welcome to the
1108 Tidyverse. *Journal of Open Source Software*, 4(43), 1686. <https://doi.org/10.21105/joss.01686>
- 1109 Wilming, N., Betz, T., Kietzmann, T. C., & König, P. (2011). Measures and Limits of Models of
1110 Fixation Selection. *PLoS ONE*, 6(9), e24038. <https://doi.org/10.1371/journal.pone.0024038>
- 1111 Wu, C.-C., Wick, F. A., & Pomplun, M. (2014). Guidance of visual attention by semantic
1112 information in real-world scenes. *Frontiers in Psychology*, 5(FEB).
1113 <https://doi.org/10.3389/fpsyg.2014.00054>
- 1114 Yarbus, A. L. (1967). *Eye Movements and Vision*. Plenum Press.
- 1115 Zelinsky, G. J., & Bisley, J. W. (2015). The what, where, and why of priority maps and their
1116 interactions with visual working memory. *Annals of the New York Academy of Sciences*, 1339(1),
1117 154–164. <https://doi.org/10.1111/nyas.12606>